Appl Microbiol Biotechnol (2013) 97:5013–5026
DOI 10.1007/s00253-013-4718-z

Metabolic fluxes in *Schizosaccharomyces pombe* grown on glucose and mixtures of glycerol and acetate

Tobias Klein · Elmar Heinzle · Konstantin Schneider

Received: 29 November 2012 / Revised: 13 January 2013 / Accepted: 14 January 2013 / Published online: 7 February 2013

Abstract Growth on glycerol has already been a topic of research for several yeast species, and recent publications deal with the regulatory mechanisms of glycerol assimilation by the fission yeast *Schizosaccharomyces pombe*. We investigated glycerol metabolism of *S. pombe* from a physiological point of view, characterizing growth and metabolism on a mixture of glycerol and acetate and comparing it to growth on glucose under respirative growth conditions in chemostat experiments. On glycerol/acetate mixtures, the cells grew with a maximum specific growth rate of 0.11 h^{-1} where 46 % of the carbon was channeled into biomass and the key fermentation product ethanol was not detectable. ^{13}C-assisted metabolic flux analysis resolved substrate distributions through central carbon metabolism, proving that glycerol is used as a precursor for glycolysis, gluconeogenesis, and the pentose phosphate pathway, while acetate enters the tricarboxylic acid cycle via acetyl-CoA. Considering compartmentalization between cytosol and mitochondria in the metabolic model, we found compartmentalization of biosynthesis for the amino acids aspartate and leucine. Balancing of redox cofactors revealed an abundant production of cytosolic NADPH that must be finally regenerated via the respiratory chain shown by the simulated and measured CO_2 production and oxygen consumption rates which were in good agreement.

Keywords Glycerol/acetate · *Schizosaccharomyces pombe* · Physiology · [^{13}C] metabolic flux analysis · Compartmentalization · Redox balancing

T. Klein · E. Heinzle · K. Schneider (✉)
Biochemical Engineering Institute, Saarland University, Campus A1.5,
66123, Saarbrücken, Germany
e-mail: ko.schneider@mx.uni-saarland.de

Introduction

With the numbers of bio-based industrial processes continuously increasing, the need for renewable feedstock is rising in order to guarantee the sustainability of these processes for the years to come. Crude glycerol, a waste product from biodiesel production, has come to attention recently as an affordable and widely available carbon source for microbial bioprocesses (Dobson et al. 2012; Rumbold et al. 2010). Various prokaryotic and eukaryotic microorganisms are able to use glycerol as carbon source (Dobson et al. 2012) and its successful application for the industrially relevant yeasts *Saccharomyces cerevisiae* and *Pichia pastoris* has been described (Ferreira et al. 2012; Yu et al. 2012). Recently, the utilization of glycerol as carbon source and the underlying regulatory network in the fission yeast *Schizosaccharomyces pombe* have come into the focus of research. In contrast to other yeasts, *S. pombe* is unable to grow on glycerol as sole carbon source (Matsuzawa et al. 2010). The first steps of glycerol metabolization in *S. pombe* involve the oxidation to dihydroxyacetone (DHA) via glycerol dehydrogenase (GlyDH), encoded by *gld1*, and further phosphorylation via DHA kinase, encoded by the genes *dak1* and *dak2*, to dihydroxyacetone phosphate (DHAP) (Matsuzawa et al. 2010). These genes as well as the gene for fructose 1,6-bisphosphatase (FBPase) *fbp1* are subject to glucose catabolite repression (Matsuzawa et al. 2012a, b). Glycerol itself does not induce expression of these key enzymes (Matsuzawa et al. 2012b), explaining to some extent the inability of *S. pombe* to grow on glycerol as sole carbon source. Instead, expression of these genes is induced by the addition of ethanol or isopropanol to the media (Matsuzawa et al. 2012b). C_2 bodies like ethanol cannot serve as sole carbon source for *S. pombe* due to the absence of a functional glyoxylate cycle (de Jong-Gubbels et al. 1996), as well as phosphoenolpyruvate carboxykinase

(PEPCK) (Rhind et al. 2011), the enzyme catalyzing the first step of gluconeogenesis. However, ethanol can be metabolized in combination with another carbon source like glucose (de Jong-Gubbels et al. 1996) or glycerol (Matsuzawa et al. 2010) and growth of *S. pombe* on mixtures of glycerol and acetate has been described recently (Klement et al. 2011).

Although *S. pombe* is primarily known as model organism for molecular and cellular biology, its use for the production of metabolites (Hansen et al. 2009; Neunzig et al. 2012) and recombinant proteins (Celik and Calik 2011; Mukaiyama et al. 2010) has been demonstrated and *S. pombe* is regarded as a potential cell factory especially for the recombinant production of mammalian proteins (Celik and Calik 2011). Thus, the efficient utilization of an affordable carbon source like glycerol is of interest. While the regulatory network of glycerol metabolism has been investigated in detail, little information is available describing this metabolism from a more physiological point of view. In this study, we cultivated *S. pombe* on a mixture of glycerol and acetate, showing that growth on this mixture is respirative. Depending on the purpose, e.g., recombinant protein production, this can be an important advantage compared to fermentative carbon sources like glucose, since no carbon is lost via fermentative pathways. We determined important physiological parameters of growth on the glycerol/acetate mixture and compared them to respirative growth on glucose. To get an overview of active metabolic pathways, activities of several key enzymes were determined on both glucose and a mixture of glycerol/acetate. We used ^{13}C tracer studies to get an insight into the contribution of both substrates to the central carbon metabolism. Metabolic flux analysis was applied to determine the flux distributions through central carbon metabolism in cells grown on glucose and on glycerol/acetate and allowed the differentiation between cytosolic and mitochondrial acetyl-CoA formation, while in addition, pointing towards compartmentation of certain pathways of amino acid biosynthesis. Further, we observed an abundant production of cytosolic NADPH on both glucose and glycerol/acetate which is eventually reoxidized via the respiratory chain by a mechanism yet unidentified.

Materials and methods

Strains and media

All cultivation experiments were performed with *S. pombe* wild-type strain 972h- (ATCC 24843). For growth on glycerol/acetate mixtures, a minimal media was used consisting of glycerol, 9.3 gL^{-1}; sodium acetate, 4.1 gL^{-1}; NH_4SO_4, 15.0 gL^{-1}; KH_2PO_4, 11.0 gL^{-1}; $MgCl_2$, 1.0 gL^{-1}; NaCl, 1.0 gL^{-1}; and $CaCl_2$, 14.0 mgL^{-1}. Vitamins and minerals were added to the following final concentrations: calcium pantothenate, 1.0 mgL^{-1}; nicotinic acid, 10.0 mgL^{-1}; myo-inositol, 10.0 mgL^{-1}; pyridoxine, 0.5 mgL^{-1}; biotin, 0.01 mgL^{-1}; $FeSO_4$, 0.7 mgL^{-1}; $ZnSO_4$, 0.8 mgL^{-1}; $MnSO_4$, 0.8 mgL^{-1}; boric acid, 1.0 mgL^{-1}; $CoCl_2$, 1.0 mg L^{-1}; $NaMoO_4$, 5.0 mgL^{-1}; potassium iodide, 2.0 mgL^{-1}; and $CuSO_4$, 0.08 mgL^{-1}. The pH of the media was set to 5.5. For chemostat cultivations on glucose, a previously described medium was used (Klein et al. 2012).

Cultivation conditions

Shake flask cultivations were performed in baffled shake flasks at 30 °C and 230 rpm. Fermentations were performed in a Vario 1000 bioreactor with 100 ml working volume (Meredos, Bovenden, Germany) at 30 °C and a stirring rate of 1,000 min^{-1}. The aeration rate was controlled at 100 ml min^{-1} using a mass flow controller (WMR Compact 4, Brooks Instruments, Veenendal, Netherlands). Temperature, stirring speed, and pH were controlled by an FCE 03 control unit (FairMenTec, Wald, Switzerland). To avoid foaming, 100 μlL^{-1} media of antifoam reagent (Antifoam 289, Sigma-Aldrich, Taufkirchen, Germany) was added. Continuous cultivation experiments with glucose were performed in the previously described system of 10-ml scale parallel bioreactors at a dilution rate D=0.1 h^{-1} (Klein et al. 2012). For tracer studies, naturally labeled substrates were exchanged for [1,3-^{13}C] glycerol, [1,2-^{13}C] sodium acetate, and [1-^{13}C] glucose which were purchased from Cambridge Isotope Laboratories (Andover, MA, USA). All labeled substances had a purity of 99.0 %.

Cell disruption and quantification of in vitro enzyme activities

For in vitro enzyme activity assays, cells were grown in 25 ml of minimal media containing glycerol and acetate and harvested in the mid-exponential phase, resulting in a biomass concentration between 1.8 and 2.4 g cell dry weight (CDW)L^{-1}. For enzyme assays from glucose chemostat cultures, the whole culture was harvested, resulting in a biomass concentration of 1.2 to 1.3 g CDWL^{-1}. Preparation of cell extracts and determination of protein concentration were performed as described previously (de Jong-Gubbels et al. 1995). Enzyme assays for pyruvate carboxylase (PYC), PEPCK, pyruvate decarboxylase (PDC), phosphofructokinase (PFK), and FBPase were performed according to the method of de Jong-Gubbels et al. (1996). Assays for dehydrogenases were performed in a 100-mM Tris–HCl buffer with pH 8.0, containing 1 mM $MgCl_2$, 1 mM of the cofactors NAD^+ or $NADP^+$, and the following substrate concentrations: glycerol, 50 mM; acetaldehyde, 10 mM; glucose-6-phosphate, 10 mM; sodium

glutamate, 50 mM; isocitrate trisodium salt, 10 mM. The final volume of the assays was 1 ml. Each assay contained an appropriate amount of cell extract and was started by the addition of the corresponding substrate. The progression of the absorption at 340 nm was monitored photometrically at 30 °C over 15 to 30 min and the enzyme activities were calculated. All determinations were performed in triplicates.

Analytics of culture supernatants and off-gas

For the calculation of consumption and production rates of metabolites on glycerol/acetate, culture samples were taken during the exponential growth phase and analysis of culture supernatants and off-gas was performed as described previously (Klein et al. 2012). In case of chemostat cultivations in the small-scale bioreactor system, the whole reactor was harvested for analysis of culture supernatants. A correlation between CDW and optical density (OD) at 595 nm was determined to be $OD_{595}=0.60$ g $CDW L^{-1}$ for growth on glycerol/acetate mixtures. The correlation for growth on glucose with $OD_{595}=0.62$ g $CDW L^{-1}$ was taken from Klein et al. (2012).

Analysis of ^{13}C labeling in proteinogenic amino acids and fatty acids

Samples from shake flask cultures of *S. pombe* cells grown on ^{13}C-labeled glycerol or acetate were taken during mid-exponential phase. To ensure isotopic steady state, samples were taken at three different biomass concentrations. Metabolic steady state was confirmed by constant rates for substrate uptake and product formation. In case of chemostat experiments, cells were cultured for five residence times after switching to [1-^{13}C] glucose. Samples were taken from the bioreactor outlets and a final sample by harvesting the bioreactor. Cells were sampled by centrifugation at 13,000×*g* at 4 °C for 3 min. For the extraction of amino acids from the cellular protein, the cell pellet was washed twice with distilled water, resuspended in 100 µl of 6 M HCl, and incubated for 24 h at 100 °C for hydrolysis of the cellular protein. Gas chromatography–mass spectrometry (GC-MS) measurement of the proteinogenic amino acids was carried out as described by Frick and Wittmann (2005). For fatty acid analysis, a method was used for extraction and direct transesterification of lipogenic fatty acids derived from biomass (Rodriquez-Ruiz et al. 1998). GC-MS analysis of fatty acid methyl esters was performed by applying a GC-MS method described by Schneider et al. (2009). The labeling distribution of stearic acid was analyzed and used to determine the ratio of acetyl-CoA derived from glycerol and from acetate. Table 1 depicts the amino acid and fatty acid fragments which were chosen for quantifying the ^{13}C enrichment for ^{13}C metabolic flux analysis.

Metabolic network and metabolic flux analysis

The metabolic network comprised glycolysis, pentose phosphate pathway (PPP), and citrate cycle as well as anabolic reactions for amino acid synthesis. The stoichiometric model and reaction reversibilities are shown in Table 2. The anabolic demand for biomass formation was adapted from the *S. cerevisiae* model of Gombert et al. (2001) and is shown in Table 3. Cytosol and mitochondria were implemented as separate compartments with separate pools for pyruvate, acetyl-CoA, oxaloacetate (OAA), and malate. Amino acid biosyntheses were assumed to be carried out in one compartment, except the formation of alanine, leucine, and aspartate which were allowed in both compartments. Extracellular fluxes were the substrate uptake vinpGlc for growth on glucose as well as vinpGly and vinpAc for growth on glycerol/acetate. On both substrates, secretion of small amounts of pyruvate (vext1) and succinate (vext2) was considered. The model contained an unbalanced pool of methyltetrahydrofolate (MTF), allowing the transfer of C_1 bodies for glycine and methionine biosynthesis. CO_2 production rate was left variable but closed balances with a maximum error of 5 % for carbon and degree of reduction were applied as constraints. Produced NAD(P)H that was not consumed for biosynthesis was regenerated via the respiratory chain with oxygen as terminal electron acceptor. For balancing of intracellular metabolite pools, the following balance equations were defined:

Cytosolic metabolite pools

1. (a) For growth on glucose: glucose-6-phosphate: vinpGlc−v1−v14−vb1=0
   (b) For growth on glycerol/acetate: glucose-6-phosphate: v1−v14−vb1=0
2. Fructose 6-phosphate: v1−v2+v16+v17=0
3. Glyceraldehyde 3-phosphate (GAP): v2−v3−v4−vb4=0
4. (a) For growth on glucose: DHAP: v2−v3=0
   (b) For growth on glycerol/acetate: DHAP: vinpGly −v3−v2=0
5. 3-Phosphoglycerate (3PG): v4−v5−v27−vb5=0
6. Phosphoenolpyruvate: v5−v6−v34−v38−vb6=0
7. Cytosolic pyruvate: v6−v7+v12−v13−v24−v35−vext1=0
8. Acetaldehyde: v24−v25+v32=0
9. (a) For growth on glucose: acetate: v25−v26=0
   (b) For growth on glycerol/acetate: v25+vinpAc−v26=0
10. Cytosolic acetyl-CoA: v26−v9−vb7−v44=0
11. Cytosolic OAA: v13−v8−v29=0
12. Cytosolic malate: v11−v12=0
13. Pentose phosphate: v14−v15−v17−vb2=0
14. Erythrose-4-phosphate: v16−v17−v34−vb3=0
15. Sedoheptulose-7-phosphate: v15−v16=0

Table 1 Fragments of amino acids and fatty acids measured by GC-MS for determination of labeling patterns

Metabolite	Measured fragments (*m/z*)	Carbon atoms from precursor
Alanine	260	1–2–3
Glycine	246	1–2
Valine	288	1–2–3–4–5
Leucine	200	2–3–4–5–6
Isoleucine	200	2–3–4–5–6
Serine	390	1–2–3
Threonine	404	1–2–3–4
Phenylalanine	336	1–2–3–4–5–6–7–8–9
Aspartate	418	1–2–3–4
Glutamate	432	1–2–3–4–5
Stearic acid	143	–2–3–4–5–6–7–8

16. Shikimate-5-phosphate: v34−v38=0
17. Cytosolic 2-oxoisocaproate: v44−v45=0
18. Glutamate: v39−vb10=0
19. Cytosolic aspartate: v29−v31−v41−v50=0
20. Mixed aspartate pool: v49+v50−vb11=0
21. Serine: v27−v28−vb12=0
22. Glycine: v28+v32−vb13=0
23. Threonine: v31−v32−v40−vb14=0
24. Phenylalanine: v38−vb15=0
25. Valine: v37−vb16=0
26. Isoleucine: v40−vb19
27. Methionine: v41−vb18=0
28. Lysine: v48−vb20=0
29 Alanine: v35+v36−vb9=0
30. Leucine: v43+v45−vb19=0
31. (a) For growth on glucose: NAD(P)H: v4+v10+v12+v14+v19+v20+v21+v23+v32+v42+v44−v31−v33−v34−v39−v40−v41−vb22=0
    (b) for growth on glycerol/acetate: NAD(P)H: vinpGly+v4+v10+v12+v14+v19+v20+v21+v23+v32+v42+v44−v31−v33−v34−v39−v40−v41−vb22=0

Mitochondrial metabolite pools

32. Mitochondrial pyruvate: v37−v10−v36−v40=0
33. Mitochdonrial acetyl-CoA: v9+v10−v18−v42−v46=0
34. Mitochondrial isocitrate: v18−v19=0
35. Mitochondrial 2-oxoglutarate: v19−v20−v39−v46−v49−vb8=0
36. Mitochondrial succinate: v20−v21−vext2=0
37. Mitochondrial fumarate: v21−v22=0
38. Mitochondrial malate: v22−v23−v11=0
39. Mitochondrial OAA: v23+v8−v18−v30=0
40. Mitochondrial aspartate: v30−v49=0
41. Mitochondrial 2-oxoisovalerate: v33−v37−v42=0
42. Mitochondrial 2-oxoisocaproate: v42−v43=0
43. 2-oxaloglutarate: v46−v47=0
44. 2-oxoadiapate: v47−v48=0

Calculation of metabolic fluxes was performed by fitting simulated mass isotopomer distributions to experimentally determined labeling distributions in amino acids of hydrolyzed cellular protein. Mathematical modeling and metabolic flux analysis were performed using Matlab Version 7.7.0 (Mathworks Inc., Nattick, MA, USA) as described by Yang et al. (2008). Correction of mass isotopomers for naturally occurring isotopes in the amino acid fragments and the derivatization reagent was performed as described previously (van Winden et al. 2002; Wittmann and Heinzle 1999; Yang et al. 2009). Statistical analysis was carried out applying 100 independent Monte Carlo runs.

Results

Physiology of *S. pombe* during growth on mixtures of glycerol and acetate and during respirative growth on glucose

Cells of *S. pombe* were grown in minimal media containing glycerol or acetate as sole carbon source or a mixture of both glycerol and acetate. Cell growth was only observed when cells were grown on a mixture of both substrates (Fig. 1). Growth on this mixture was characterized by a specific growth rate μ of 0.11±0.00 h^{-1} and a biomass yield of 11.39±0.05 g $Cmol^{-1}$ substrate. Glycerol and acetate were consumed simultaneously, with a specific glycerol uptake rate of 2.57±0.08 mmol g $CDW^{-1}h^{-1}$ and a specific acetate uptake rate of 0.72±0.02 mmol g $CDW^{-1}h^{-1}$ (Table 4). Ethanol as main indicator of fermentative growth was absent and only very small amounts of pyruvate and succinate of were detected in the culture supernatants.

A specific oxygen uptake rate of 4.76±0.10 mmol g $CDW^{-1}h^{-1}$ and a specific carbon dioxide production rate of 4.81±0.13 mmol g $CDW^{-1}h^{-1}$ were determined, resulting in a respiratory quotient (RQ) of 1.01. The high biomass yield and the absence of ethanol and other reduced by-products were strong indicators for respirative growth of *S. pombe* on glycerol/acetate mixtures. A closed carbon balance (carbon recovery 97 %) assured the consideration of all relevant extracellular carbon fluxes. Chemostat cultivations of *S. pombe* on glucose under respirative growth conditions (D= 0.1 h^{-1}) resulted in a slightly increased biomass yield of 14.73 ±0.19 g $Cmol^{-1}$ substrate compared to glycerol/acetate grown cells (Table 4). Cells grown respiratively on glucose exhibited a reduced CO_2 production rate of 2.75±0.04 mmol g CDW^{-1} h^{-1} compared to glycerol/acetate grown ones, pointing

Table 2 Stoichiometric network used for metabolic flux analysis

Name	Reaction stoichiometry		
v1	Glucose-6-P	↔	Fructose-6-P
v2	Fructose-6-P	↔	Glycerolaldehyde-3-P+dihydroxyacetone-P
v3	Glycerolaldehyde-3-P	↔	Dihydroxyacetone-P
v4	Glycerolaldehyde-3-P	→	3-Phosphoglycerate
v5	3-Phosphoglycerate	→	Phosphoenolpyruvate
v6	Phosphoenolpyruvate	→	Cyt. pyruvate
v7	Cyt. pyruvate	→	Mit. pyruvate
v8	Cyt. oxaloacetate	↔	Mit. oxaloacetate
v9	Cyt. acetyl-CoA	→	Mit. acetyl-CoA
v10	Mit. pyruvate	→	Mit. acetyl-CoA+CO_2
v11	Mit. malate	→	Cyt. malate
v12	Cyt. malate	→	Cyt. pyruvate+CO_2
v13	Cyt. pyruvate	→	Cyt. oxaloacetate
v14	Glucose-6-P	→	Pentose-P+CO_2
v15	2 Pentose-P	↔	Sedoheptulose-5-P+glycerolaldehyde-3-P
v16	Sedoheptulose-5-P+glycerolaldehyde-3-P	↔	Fructose-6-P+erythrose-4-P
v17	Pentose-P+erythrose-4-P	↔	Fructose 6-phosphate+glycerolaldehyde-3-P
v18	Mit. oxaloacetate+mit. acetyl-CoA	→	Mit. isocitrate
v19	Isocitrate	→	2-Oxoglutarate+CO_2
v20	2-Oxoglutarate	→	Succinate+CO_2
v21	Succinate	→	Fumarate
v22	Fumarate	→	Mit. malate
v23	Mit. malate	→	Mit. oxaloacetate
v24	Cyt. pyruvate	→	Acetaldehyde
v25	Acetaldehyde	→	Acetate
v26	Acetate	→	Cyt. acetyl-CoA
v27	3-Phosphoglycerate	→	Serine
v28	Serine	↔	Glycine+MTF
v29	Cyt. oxaloacetate	→	Cyt. aspartate
v30	Mit. oxaloacetate	→	Mit. aspartate
v31	Cyt. asparate	→	Threonine
v32	Threonine	↔	Glycine+acetaldehyde
v33	Mit. pyruvate	→	Oxoisovalerate
v34	Phosphoenolpyruvate+erythrose-4-P	→	Shikimate-5-P
v35	Cyt. pyruvate	→	Alanine
v36	Mit. pyruvate	→	Alanine
v37	2-Oxisovalerate	→	Valine
v38	Phosphoenolpyruvate+shikimate-5-P	→	Phenylalanine+CO_2
v39	2-Oxoglutarate	→	Glutamate
v40	Threonine+mit. pyruvate	→	Isoleucine+CO_2
v41	Cyt. aspartate+MTF	→	Methionine
v42	2-Oxoisovalerate+mit. acetyl-CoA	→	Mit. 2-oxoisocaproate+CO_2
v43	Mit. 2-oxoisocaproate	→	Leucine
v44	2-Oxoisovalerate+cyt. acetyl-CoA	→	Cyt. 2-oxoisocaproate+CO_2
v45	Cyt. 2-oxoisocaproate	→	Leucine
v46	Mit. 2-oxoglutarate+mit. acetyl-CoA	→	Mit. oxaloglutarate
v47	Mit. oxaloglutarate	→	Mit. 2-oxoadipate+CO_2
v48	Mit. 2-oxoadipate	→	Lysine
v49	Mit. aspartate	→	Aspartate

Table 2 (continued)

Name	Reaction stoichiometry		
v50	Cyt. aspartate	→	Aspartate
vext1	Cyt. pyruvate	→	Ext. pyruvate
vext2	Mit. succinate	→	Ext. succinate
vinp Glc	Ext. glucose	→	Glucose-6-P
vinp Gly	Ext. glycerol	→	Dihydroxyacetone-P
vinp Ac	Ext. acetate	→	Cyt. acetate
vb1	Glucose-6-P	→	Biomass
vb2	Pentose-P	→	Biomass
vb3	Erythrose-4-P	→	Biomass
vb4	Glycerol-aldehyde-3-P	→	Biomass
vb5	3-Phosphoglycerate	→	Biomass
vb6	Phosphoenolpyruvate	→	Biomass
vb7	Cyt. acetyl-CoA	→	Biomass
vb8	Mit. 2-oxoglutarate	→	Biomass
vb9	Alanine	→	Biomass
vb10	Glutamate	→	Biomass
vb11	Aspartate	→	Biomass
vb12	Serine	→	Biomass
vb13	Glycine	→	Biomass
vb14	Threonine	→	Biomass
vb15	Phenylalanine	→	Biomass
vb16	Valine	→	Biomass
vb17	Isoleucine	→	Biomass
vb18	Methionine	→	Biomass
vb19	Leucine	→	Biomass
vb20	Lysine	→	Biomass
vb21	CO_2	→	Biomass
vb22	Cofactor	→	Biomass

Arrows indicate direction of reaction and reversible reactions

Cyt. cytosolic, *Mit.* mitochondrial, *Ext.* external, *P* phosphate residue, *MTF* unbalanced pool of methyltetrahydrofolate

towards a significant increase of CO_2 producing fluxes during growth on the glycerol/acetate mixture. On glucose, the specific oxygen consumption rate matched the specific CO_2 production rate, resulting in an RQ value of 1.02.

Quantification of in vitro enzyme activities on glycerol/acetate mixtures and glucose

In vitro enzyme activities of several key enzymes of central carbon metabolism, namely, glucose-6-phosphate dehydrogenase (G6PDH), PFK, FBPase, GlyDH, PDC, PYC, acetaldehyde dehydrogenase (AADH), PEPCK, and isocitrate dehydrogenase (IcDH), were quantified in order to set up the stoichiometric model applied for metabolic flux analysis. Enzyme assays were performed using cells grown on mixtures of glycerol/acetate as well as cells from glucose chemostat cultures grown at a dilution rate of 0.1 h^{-1}. Specific activities of all enzymes were similar on both substrates except for FBPase. Cells grown on glycerol/acetate mixtures exhibited a specific enzyme activity of 0.58± 0.06 Umg^{-1}, whereas no activity for FBPase was observed in extracts of glucose-grown cells. In addition, no activity for PEPCK was detectable on both substrates. GlyDH activity was observed on both substrates with a specific enzyme activity of 0.71±0.05 Umg^{-1} on the glycerol/acetate mixture and 0.50±0.01 Umg^{-1} on glucose (Table 5).

Distribution of acetate throughout the central carbon metabolism

In order to verify the activity of the different central metabolic pathways and the distribution of the substrates glycerol and acetate throughout the central metabolism, especially focusing on a potential gluconeogenic flux, *S. pombe* was

Table 3 Anabolic demand for *S. pombe* during respirative growth (specific growth rate of 0.1 h^{-1})

Precursor	Demand [mmol g CDW^{-1}]
Glucose-6-phosphate	1.730
Pentose-5-phosphate	0.163
Erythrose-4-phosphate	0.153
Glyceraldehyde 3-phosphate	0.077
3-Phosphoglycerate	0.565
Phosphoenolpyruvate	0.271
Cytosolic acetyl-CoA	1.900
Mitochondrial acetyl-CoA	0.290
Alanine	0.354
Glutamate	0.639
Aspartate	0.359
Serine	0.400
Glycine	0.275
Threonine	0.243
Phenylalanine	0.130
Valine	0.232
Isoleucine	0.174
Methionine	0.042
Leucine	0.198
Lysine	0.200
Cytosolic NADPH	4.65
Mitochondrial NADPH	4.16

Data are given in millimoles per gram CDW and were adapted from Gombert et al. (2001)

cultivated on ^{13}C-labeled substrates. Based on the ^{13}C enrichment of proteinogenic amino acids, the distribution of the corresponding substrates was determined. Feeding universally labeled acetate resulted in ^{13}C enrichment in glutamate, suggesting that acetate enters the tricarboxylic acid (TCA) cycle via acetyl-CoA (Fig. 2). No enrichment of ^{13}C was observed for serine derived from 3PG and phenylalanine derived from PEP and erythrose-4-phosphate, thus pointing towards an inactive gluconeogenic flux from OAA towards PEP under the applied growth conditions using a mixture of glycerol and acetate.

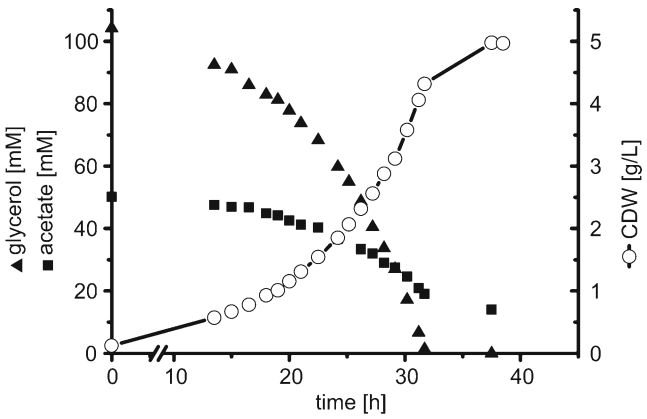

Fig. 1 Growth (*circles*) and substrate uptake of *S. pombe* grown in a minimal media containing glycerol (*filled triangles*) and acetate (*filled squares*) as carbon sources

Metabolic flux analysis on glucose and glycerol/acetate

[1-^{13}C] glucose was used as tracer substrate in chemostat cultivations of *S. pombe*. For tracer studies on glycerol/acetate mixtures, [1,3-^{13}C] glycerol was used as well as [1,2-^{13}C] acetate. Flux simulations were performed with tracer information from [1,2-^{13}C] acetate, [1,3-^{13}C] glycerol, and a combination of both tracer experiments. The combined approach consisted of two experiments (^{13}C-labeled acetate/naturally labeled glycerol and vice versa) where both datasets were used in parallel to obtain the flux distribution. The flux distributions from this combined approach were used for comparison with flux distributions in glucose limited chemostats.

Metabolic fluxes during growth on glucose are depicted in Fig. 3a, corresponding fluxes during growth on the glycerol/acetate mixture are shown in Fig. 3b. A strong activity of the TCA cycle was observed on both substrates. IcDH activity was identical under both cultivation conditions, exhibiting a flux of 0.79±0.03 mmol g $CDW^{-1}h^{-1}$ on glucose and 0.78±0.04 mmol g $CDW^{-1}h^{-1}$ on the glycerol/acetate mixture.

In case of the glycerol/acetate substrate mixture, measurement of the labeling pattern of stearic acid allowed a good resolution of the flux distributions around the pyruvate node. Acetate taken up from the media was the main source of cytosolic acetyl-CoA synthesized by acetyl-CoA synthethase. Only a fraction of 26.5 % of cytosolic acetyl-CoA was produced by decarboxylation of cytosolic pyruvate. Cytosolic acetyl-CoA (0.20 mmol g $CDW^{-1}h^{-1}$) was used for biosynthesis, while most of it was transported into the mitochondria. In contrast, the flux via the pyruvate dehydrogenase complex synthesizing mitochondrial acetyl-CoA form mitochondrial pyruvate was very small and, therefore, hard to determine precisely.

A clear compartmentation of leucine biosynthesis was observed in *S. pombe* which was found to use exclusively mitochondrial acetyl-CoA for the synthesis of leucine. The stoichiometric model involved a mitochondrial and a cytosolic biosynthetic route for leucine. However, the flux for mitochondrial leucine production was 0.017±0.00 mmol g $CDW^{-1}h^{-1}$, whereas for cytosolic leucine, a production flux of 0.00±0.00 mmol g $CDW^{-1}h^{-1}$ was determined. Further, aspartate and thus threonine were synthesized exclusively from cytosolic OAA during growth on both substrates, while no incorporation of mitochondrial OAA was observed. A compartmentation for alanine biosynthesis could not be determined but was assumed to take place in the mitochondria (see the "Discussion" section).

Table 4 Physiological parameters of growth of *S. pombe* on a mixture of glycerol and acetate compared to cultivations on glucose under respirative conditions (D=0.1 h^{-1})

Substrate	$Y_{X/S}$ [g Cmol^{-1}]	q_s [mmol$g^{-1}h^{-1}$]		q_{O2} [mmol$g^{-1}h^{-1}$]	q_{CO2} [mmol$g^{-1}h^{-1}$]	RQ
		q_{gly}	q_{ac}			
Glycerol/acetate	11.39±0.05	2.57±0.08	0.72±0.02	4.76±0.13	4.81±0.10	1.01
Glucose	14.73±0.19	1.08±0.05		2.69±0.11	2.75±0.04	1.02

Standard deviations were obtained from two parallel experiments

On glucose and the glycerol/acetate mixture, a net flux from cytosolic OAA to mitochondrial OAA was observed. On glycerol/acetate mixtures, the flux from cytosolic OAA to mitochondrial OAA was 0.18±0.01 mmol$g\ CDW^{-1}h^{-1}$, while the reverse flux was 0.02±0.00 mmol$g\ CDW^{-1}h^{-1}$, resulting in a net flux of 0.16±0.01 mmol$g\ CDW^{-1}h^{-1}$ with a reversibility ζ of 0.14. On glucose, the reversibility of this import could not be determined. However, the net flux from cytosolic OAA towards mitochondrial OAA was 0.34± 0.05 mmol$g\ CDW^{-1}h^{-1}$ and thus two times higher compared to growth on glycerol/acetate mixtures. At the same time, the export from mitochondrial malate into the cytosol and pyruvate production from cytosolic malic enzyme was 10 times higher on glucose than on glycerol/acetate mixtures.

Glycerol is metabolized via the formation of DHAP in the first two steps, which is further converted to GAP. At this point, GAP is either condensed with DHAP for the formation of fructose 6-phosphate or channeled into glycolysis with pyruvate as end product. During growth on glycerol/acetate mixtures, the major demand for acetyl-CoA is covered by acetate supplied via the media. This demand must be completely met by the formation of acetyl-CoA from pyruvate during growth on glucose. Thus, the flux from GAP to pyruvate was 1.8 times higher on glucose than on glycerol/acetate mixtures. The remaining glycerol followed the gluconeogenic route towards fructose 6-phosphate with a flux of 1.50 mmol$g\ CDW^{-1}h^{-1}$. A high flux through the nonoxidative part of the PPP, generating additional fructose 6-phosphate increased the flux towards glucose 6-phosphate to 4.07 mmol$g\ CDW^{-1}h^{-1}$. Respirative growth on glucose lead to a flux of 0.69 mmol $g\ CDW^{-1}h^{-1}$ of glucose 6-phosphate to the pentose 5-phosphates, generating 1.38 mmol$g\ CDW^{-1}h^{-1}$ of cytosolic NADPH. The flux through the oxidative PPP on the glycerol/acetate mixture was 5.6 times higher (3.89 mmol$g\ CDW^{-1}h^{-1}$), generating 7.78 mmol$g\ CDW^{-1}h^{-1}$ of cytosolic NADPH. The fluxes through the nonoxidative part of the PPP were increased by the same factor accordingly, generating the previously mentioned high back flux towards fructose 6-phosphate. Thus, the carbon atoms of glycerol were cycled through the PPP, generating increased amounts of CO_2 which is in good agreement with the increased carbon dioxide production rate of 4.81±0.10 mmol$g\ CDW^{-1}h^{-1}$ observed as well as a vast increase of the cytosolic NADPH production.

Balancing of redox cofactors

Rates for production and consumption of NADH and NADPH as well as CO_2 and oxygen were calculated from the flux simulation datasets. These data were used to review the accuracy of metabolic flux analysis by comparing the calculated values with the experimental data from off-gas analysis.

Cofactor specificities of the key dehydrogenases of the central carbon metabolism were determined along with the enzyme activity assays. Only G6PDH showed cofactor specificity for $NADP^+$, all other dehydrogenases tested exhibited activity with both cofactors (NAD^+/$NADP^+$) (Table 5).

Table 5 Specific enzyme activities [in units per milligram] for key enzymes of the central carbon metabolism for cells grown on glucose in chemostat at D=0.1 h^{-1} and on the glycerol/acetate mixture. For dehydrogenases, activities were determined with both NAD^+ and $NADP^+$. *n.d.* not detectable

	Glucose, D=0.1 h^{-1}			Glycerol/acetate mixture		
PFK			0.73±0.06			0.68±0.02
FBPase			n.d.			0.58±0.06
PDC			0.21±0.02			0.14±0.01
PYC			0.12±0.01			0.14±0.01
PEPCK			n. d.			n. d.
	NAD^+	$NADP^+$	Total	NAD^+	$NADP^+$	Total
G6PDH	n.d.	1.25±0.12	1.25±0.12	0.0	1.14±0.04	1.14±0.04
GlyDH	0.34±0.01	0.17±0.01	0.50±0.01	0.51±0.04	0.20±0.02	0.71±0.05
AADH	0.02±0.0	0.08±0.0	0.1±0.0	0.05±0.01	0.08±0.01	0.13±0.01
IcDH	0.07±0.0	0.12±0.01	0.19±0.01	0.10±0.02	0.56±0.04	0.66±0.04

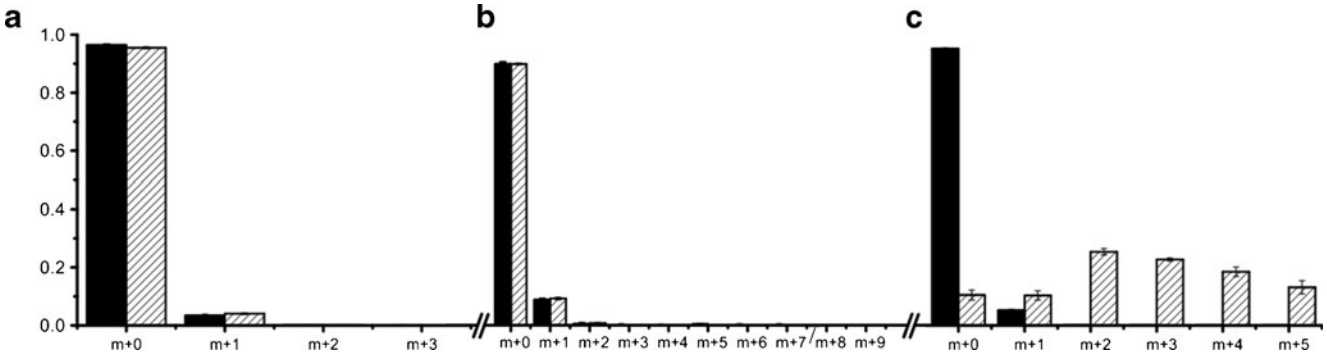

Fig. 2 Mass distribution vectors (MDVs) of selected proteinogenic amino acids from cultivations on glycerol and acetate. *Filled bars* show MDVs from cultivations on unlabeled substrates, *hatched bars* show MDVs from cultivations with [1,2-^{13}C] acetate. **a** Serine; **b** phenylalanine; **c** glutamate. *Error bars* indicate standard deviations

The oxidative PPP was considered as sole source of cytosolic NADPH. Considering the anabolic demand for NADPH (Table 3) as well as NADPH-consuming reactions in the metabolic model (Table 2), the flux through the oxidative PPP produced a surplus of cytosolic NADPH of 0.66 mmol g CDW^{-1} h^{-1} on glucose and 6.96 mmol g CDW^{-1} h^{-1} on glycerol/acetate. In *S. pombe*, AADH is encoded by only one gene, SPAC9E9.09c, and the enzyme is localized in the cytosol (Matsuyama et al. 2006). Thus, IcDH was considered as the only source of mitochondrial NADPH production. Since mitochondrial IcDH exhibited activity for both NAD$^+$ and NADP$^+$, the NADPH production was assumed to match the mitochondrial NADPH demand. AADH was considered to produce only NADH, since the PPP already produced a surplus of cytosolic NADPH.

The NADH production rates were calculated to be 4.86 mmol g CDW^{-1} h^{-1} on glycerol/acetate and 3.14 mmol g CDW^{-1} h^{-1} on glucose respectively. Since cell growth was respirative on both substrates, NADH reoxidation should exclusively occur via the respiratory chain with a ratio of 2 mol NADH per mol O_2. Further, the surplus of cytosolic NADPH was considered to be eventually reoxidized via the respiratory chain. The calculation of a specific oxygen uptake rate as well as a CO_2 production rate from the flux data and the resulting calculated RQ values matched the experimentally determined values (Table 6). The difference from the experimentally determined values was at most 2.6 % for glucose and not more than 6.6 % for glycerol/acetate. These results strongly indicated direct or indirect reoxidation of the excess NADPH by the respiratory machinery.

Discussion

Glycerol from biodiesel production is a readily available carbon source for microbial bioprocesses. While glycerol utilization for other yeasts has been investigated in detail, little work has been performed concerning the physiology of *S. pombe* grown on glycerol. Thus, our study aimed at getting an insight into the physiology of *S. pombe* grown on a mixture of glycerol and acetate and comparing the obtained results to glucose, a standard carbon source for yeast cultivations. The physiological characterization revealed that growth on the glycerol/acetate mixture was respirative due to the absence of the key fermentative product ethanol, an RQ of 1.01 and a high biomass yield of 11.39±0.05 g C mol^{-1} substrate. Glycerol uptake was much faster than acetate uptake, with a C mol ratio of uptake of 5.59:1. For chemostat cultivations with glucose/ethanol mixtures at D=0.1 h^{-1}, a C mol ratio of the uptake for glucose and ethanol up to 2.3:1 has been described (de Jong-Gubbels et al. 1996). However, complete incorporation of ethanol into biomass was observed only for C molar rations below 6.5:1 (glucose to ethanol). Increasing the ethanol uptake by increased fractions of ethanol in the medium resulted in the formation of acetate. The authors described a limitation of ethanol converting the enzymes alcohol dehydrogenase, AADH, and acetyl-CoA synthetase as reason for the limited complete utilization of ethanol and the occurring acetate production. Accordingly, such a limitation of acetate metabolization might explain the low acetate uptake rate, compared to the glycerol uptake rate. This is in agreement with the observation that increasing amounts of acetate in the media did not further increase the acetate uptake rate (date not shown).

Comparison of these results to chemostat cultivations on glucose at a dilution rate of 0.1 h^{-1} yielded comparable results with a high biomass yield of 14.73±0.19 g C mol^{-1} substrate and the absence of ethanol as well as an RQ of 1.02. The comparable degree of reduction of glucose and the glycerol/acetate mixture with an elemental composition of CH_2O for glucose and $CH_{2.6}O$ for the glycerol/acetate mixture (based on the stoichiometry ratio of the uptake of both substrates), respectively, explains the similar RQ values on both substrates. Although the degree of reduction of the

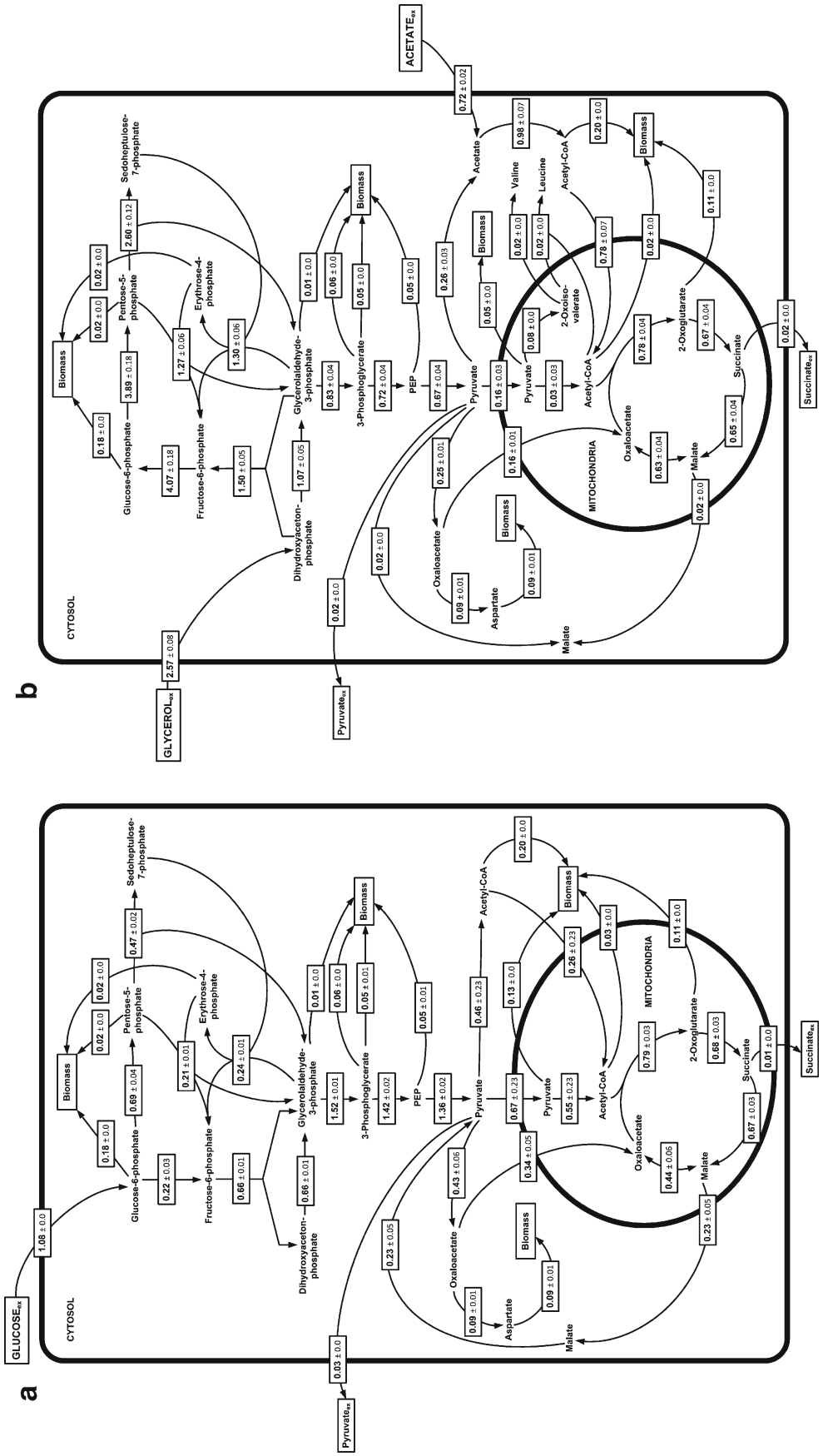

Fig. 3 Intracellular carbon flux distributions of *S. pombe*: **a** cultivated in a chemostat under respirative growth conditions (D=0.1 h^{-1}) on [1-^{13}C] glucose and **b** cultivated in a mixture of glycerol and acetate. [1,3-^{13}C] glycerol and [1,2-^{13}C] acetate were used as tracers in independent experiments. Fluxes are given in millimoles per gram CDW per hour and standard deviations are given to reflect the precision of the flux determination. For reversible reactions, net fluxes are shown and *arrows* indicate the direction of the fluxes

Table 6 Specific CO_2 production, O_2 consumption rates, and RQ values calculated from flux simulations (cal.) on glucose and the glycerol/acetate mixture compared to the experimentally determined values from off-gas analyses (exp.)

Substrate	CO_2 cal.	CO_2 exp.	O_2 cal.	O_2 exp.	RQ cal.	RQ exp.
Glucose	2.81±0.32	2.75±0.04	2.76 0.22	2.69±0.11	1.02	1.02
Glycerol/acetate	5.12±0.22	4.81±0.13	5.05±0.19	4.76±0.10	1.02	1.01

substrate mixture is increased by 15 % compared to glucose, an increased biomass yield on the glycerol/acetate mixture was not observed. This might result from an essentially altered carbon metabolism, e.g., the carbon cycling through the PPP, resulting in a substantial loss of carbon compared to glucose cultivations.

The in vitro activities of the tested enzymes of the central carbon metabolism showed similar results on both substrates. Regulation of enzyme expression in the central carbon metabolism of *S. pombe* can be strongly dependent on the growth rate and the consequent physiology (de Jong-Gubbels et al. 1996). On the other hand, expression of the tested enzymes of the central carbon metabolism seems much less dependent of the substrate since comparable growth rates and comparable physiologies are present on both substrates.

GlyDH, the first enzyme in glycerol metabolism, was also expressed when cells were grown on glucose. Chemostat cultivation applying low dilution rates resulting in respirative growth is comparable to the low glucose conditions described by Matsuzawa et al. (2010) as a condition inducing *gld1* expression, explaining the activity of GlyDH under these conditions. However, in contrast to those results, where the GlyDH was described as strictly NAD^+-dependent, we detected activity with both NAD^+ and $NADP^+$. There might be strain-specific isoenzymes or altered cofactor specificities, since we used the wild-type strain 972h-, while the strain described by Matsuzawa et al. (2010) was originally provided from Asahi Glass Co. A strong FBPase activity on glycerol/acetate in contrast to glucose-grown cells was the only remarkable difference between enzyme activities on both substrates. A strong induction in the absence of glucose and addition of ethanol has been shown before on the mRNA level (Matsuzawa et al. 2012b) and was confirmed by similar results in a direct assay of enzymatic activity (this work). These results suggest that GlyDH is a target of glucose catabolite repression and expressed if this repression disappears. The *fbp1* gene on the other hand is also repressed in the presence of glucose but expression appears to take place only upon additional induction by ethanol (Matsuzawa et al. 2012b) or acetate (this work). The enzyme assays confirmed that, on both glycerol/acetate and glucose, no activity for PEPCK could be detected which is in accordance with literature data (de Jong-Gubbels et al. 1996; Rhind et al. 2011). This result was confirmed by tracer studies with [1,2-^{13}C] acetate, showing an incorporation of ^{13}C into the amino acids derived from TCA cycle intermediates but no ^{13}C incorporation into amino acids derived from PEP or 3PG. Due to the lack of PEPCK, formation of PEP from OAA is not possible in *S. pombe*.

Metabolic flux analysis indicated highly similar TCA cycle fluxes during growth on glucose or glycerol/acetate. TCA cycle fluxes were independent of the carbon source, since growth on both substrates is respirative and the growth rates were similar. One would expect a much stronger effect by applying variations of the growth rates and switching between respirative growth and fermentative growth as shown for *S. cerevisiae* (Frick and Wittmann 2005).

On glucose, a distinction between cytosolic acetyl-CoA formation via the pyruvate dehydrogenase bypass and mitochondrial acetyl-CoA formation was not possible. Thus, no reliable statement can be made to the actual rate of pyruvate import into the mitochondria under these growth conditions. There is only a minimum import that has to take place to meet the anabolic demand for mitochondrial pyruvate, since, in contrast to *S. cerevisiae*, no mitochondrial malic enzyme can replenish the mitochondrial pyruvate pool. Likewise a minimal flux via the cytosolic pyruvate dehydrogenase bypass must be active to meet the anabolic demand for cytosolic acetyl-CoA.

Additional measurement of stearic acid labeling pattern on the glycerol/acetate mixture showed that assimilated acetate was the main source of cytosolic acetyl-CoA, while production from pyruvate via PDC made up only 26.5 % of the cytosolic acetyl-CoA pool. Most of the cytosolic acetyl-CoA was transported to the mitochondria for metabolization via the TCA cycle and, accordingly, mitochondrial acetyl-CoA production from mitochondrial pyruvate was very low and hard to determine precisely. However, leucine biosynthesis was clearly shown to use exclusively mitochondrial acetyl-CoA as precursor. The clarity of this assignment shows that there must be a slight difference in the labeling pattern between cytosolic and mitochondrial acetyl-CoA and thus a small amount of mitochondrial acetyl-CoA must be formed from mitochondrial pyruvate.

The simulation of compartmented flux distributions also gave insight into the compartmentation of biosynthesis of the amino acids aspartate and threonine. Although aspartate

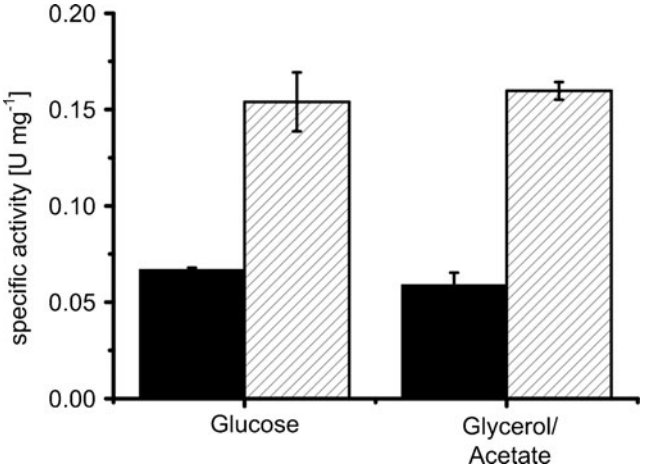

Fig. 4 Specific enzyme activities of glutamate dehydrogenases of *S. pombe* grown on glucose under respirative growth conditions (D= 0.1 h^{-1}) and on a mixture of glycerol and acetate. *Filled bars* show activity with NAD^+, *hatched bars* show activity with $NADP^+$

aminotransferases are described to be located in both cytoplasm and mitochondria of *S. pombe* (Matsuyama et al. 2006), aspartate and thus threonine were both derived solely from the cytosolic OAA pool, an observation that has been made for other yeast species but not for *S. pombe* yet (Blank et al. 2005). On both substrates, a net flux from cytosolic to mitochondrial OAA was determined. On the glycerol/acetate mixture, the reversibility of the transport could be determined with ζ=0.14, while for glucose cultivations, ζ could not be determined. However, the clear separation between cytosolic and mitochondrial aspartate biosynthesis is attributed to distinct labeling patterns of cytosolic and mitochondrial OAA pools and thus the exchange between both pools must be small on glucose. High exchange fluxes would result in basically identical labeling patterns of both OAA pools which would prevent a clear determination of compartmentalized biosynthesis of aspartate.

A separation of cytosolic and mitochondrial pools of pyruvate with [1-^{13}C] glucose has been described for *S. cerevisiae* due to differences in the labeling pattern of cytosolic pyruvate formed in the glycolysis and mitochondrial pyruvate formed by the reaction of the mitochondrial malic enzyme (Frick and Wittmann 2005). In contrast to *S. cerevisiae*, the malic enzyme of *S. pombe* is located in the cytosol (Boles et al. 1998). Here, both pyruvate pools carry the same labeling information, making it impossible to distinguish between both pools. Therefore, a separation between cytosolic and mitochondrial pyruvate pools was not possible and no information for compartmentation of alanine biosynthesis was available. Since there was no difference between the observed compartmentation of other amino acid biosyntheses in *S. pombe* and those described for *S. cerevisiae*, it seems reasonable to assume that alanine biosynthesis takes place in the mitochondria under respirative conditions as described for Baker's yeast (Frick and Wittmann 2005).

A striking difference between the two substrates was found in the CO_2 production rate. A 1.7-fold increase was observed during growth on the glycerol/acetate mixture compared to glucose-grown cells. The reason for this increase was found in a drastically increased flux through the oxidative PPP. The mixture of glycerol/acetate resulted in a sufficient supply of acetyl-CoA from acetate to meet the anabolic demands in both compartments. This led to a drastically decreased glycolytic flux towards pyruvate compared to glucose-grown cells. The flux from GAP towards pyruvate was decreased by a factor of 1.8. Since glycerol uptake was fast with a rate of 2.57 mmol g $CDW^{-1} h^{-1}$, the remaining carbon entered gluconeogenesis. This led to a cycle of the carbon atoms from glycerol through the upper part of the gluconeogenesis and the PPP, causing the observed increase in CO_2 production and raising the level of cytosolic NADPH compared to glucose cultivations. The increased carbon flux through the PPP was dictated by the ratio of glycerol and acetate derived carbon found in intermediates of the TCA cycle. Since the acetyl-CoA supplying flux from acetate is fixed, the glycolytic carbon flux from glycerol is restricted to a certain value to meet this ratio. The remaining carbon derived from glycerol uptake must be either incorporated into biomass or follow the described cycle between gluconeogenesis and PPP forming CO_2. CO_2 production rate was not used for balancing but for validation of the overall CO_2 production determined by the flux model. The good agreement between measured and simulated CO_2 production supports these findings of the carbon cycling through the PPP.

On both substrates, a surplus of cytosolic NADPH was observed, which was far more pronounced on the glycerol/acetate mixture. However, calculation of specific oxygen consumption rates and CO_2 production rates matched the experimentally determined values, if this surplus was considered to be reoxidized via the respiratory chain (Table 5). The production of excess cytosolic NADPH and its regeneration by the enzymes of the respiratory chain has been described for other yeasts like *Kluyveromyces lactis* and *Candida utilis* (Tarrio et al. 2006; Van Urk et al. 1989). No information is available on *S. pombe* and it has been clearly shown that *S. cerevisiae* is unable to reoxidize NADPH this way (Van Urk et al. 1989). Another possible explanation would be the transport of electrons from NADPH to NADH via transhydrogenase-like cycles. Their existence has been proposed by Boles et al. (1993), describing a cycle of $NAD(P)^+$-dependent glutamate dehydrogenases in *S. cerevisiae*. An upregulation of exactly these glutamate dehydrogenases has been described for mutant strains of *S. cerevisiae* which showed a relocalization of the mitochondrial $NADP^+$-dependent malic enzyme to the

cytosol (Moreira dos Santos et al. 2004). We determined in vitro activities of glutamate dehydrogenases in cells grown on the glycerol/acetate mixture and glucose and found activity for NAD^+-dependent and $NADP^+$-dependent glutamate dehydrogenases in both cases (Fig. 4). This is no real proof for the existence of such an electron-transferring cycle in *S. pombe*, but the expression of both isoforms of glutamate dehydrogenase allows such a cycle to take place in theory at least. *S. pombe* must have some means by which surplus NADPH can be regenerated via the respiratory chain. However, the mechanisms of this NADPH regeneration are yet still unclear and will be the topic of further studies.

In this study, we could show that growth of *S. pombe* on a glycerol/acetate mixture is respirative, which is an advantage compared to fermentative carbon sources like glucose in terms of reduced carbon loss and higher biomass formation. Metabolic flux analysis was used to get an insight into the metabolization of both substrates throughout the central carbon metabolism. Here, the utilization of a mixture of two substrates allowed a detailed resolution of the metabolic fluxes around the pyruvate node, which is not possible with a single carbon source like glucose in *S. pombe*. The obtained results and applied techniques can be used for further physiological studies on *S. pombe* to get a better understanding of the physiology and potential of this important microorganism.

Acknowledgments This work was supported by BMBF (Federal Ministry of Education and Research—Germany, Project SWEEPRO, FKZ 0315800B). We are very grateful for the most valuable support by Michel Fritz concerning the instrumental analysis.

References

Blank LM, Lehmbeck F, Sauer U (2005) Metabolic-flux and network analysis in fourteen hemiascomycetous yeasts. FEMS Yeast Res 5 (6–7):545–558

Boles E, Lehnert W, Zimmermann FK (1993) The role of the NAD-dependent glutamate dehydrogenase in restoring growth on glucose of a *Saccharomyces cerevisiae* phosphoglucose isomerase mutant. Eur J Biochem 217(1):469–477

Boles E, de Jong-Gubbels P, Pronk JT (1998) Identification and characterization of MAE1, the *Saccharomyces cerevisiae* structural gene encoding mitochondrial malic enzyme. J Bacteriol 180 (11):2875–2882

Celik E, Calik P (2011) Production of recombinant proteins by yeast cells. Biotechnol Adv 30(5):1108–1118

de Jong-Gubbels P, Vanrolleghem P, Heijnen S, van Dijken JP, Pronk JT (1995) Regulation of carbon metabolism in chemostat cultures of *Saccharomyces cerevisiae* grown on mixtures of glucose and ethanol. Yeast 11(5):407–418

de Jong-Gubbels P, van Dijken JP, Pronk JT (1996) Metabolic fluxes in chemostat cultures of *Schizosaccharomyces pombe* grown on mixtures of glucose and ethanol. Microbiology 142(Pt 6):1399–1407

Dobson R, Gray V, Rumbold K (2012) Microbial utilization of crude glycerol for the production of value-added products. J Ind Microbiol Biotechnol 39(2):217–226

Ferreira AR, Ataide F, von Stosch M, Dias JM, Clemente JJ, Cunha AE, Oliveira R (2012) Application of adaptive DO-stat feeding control to *Pichia pastoris* X33 cultures expressing a single chain antibody fragment (scFv). Bioprocess Biosyst Eng 35(9):1603–1614

Frick O, Wittmann C (2005) Characterization of the metabolic shift between oxidative and fermentative growth in *Saccharomyces cerevisiae* by comparative ^{13}C flux analysis. Microb Cell Fact 4:30

Gombert AK, Moreira dos Santos M, Christensen B, Nielsen J (2001) Network identification and flux quantification in the central metabolism of *Saccharomyces cerevisiae* under different conditions of glucose repression. J Bacteriol 183(4):1441–1451

Hansen EH, Moller BL, Kock GR, Bunner CM, Kristensen C, Jensen OR, Okkels FT, Olsen CE, Motawia MS, Hansen J (2009) De novo biosynthesis of vanillin in fission yeast (*Schizosaccharomyces pombe*) and Baker's yeast (*Saccharomyces cerevisiae*). Appl Environ Microbiol 75(9):2765–2774

Klein T, Schneider K, Heinzle E (2012) A system of miniaturized stirred bioreactors for parallel continuous cultivation of yeast with online measurement of dissolved oxygen and off-gas. Biotechnol Bioeng. doi:10.1002/bit.24633

Klement T, Dankmeyer L, Hommes R, van Solingen P, Buchs J (2011) Acetate–glycerol cometabolism: cultivating *Schizosaccharomyces pombe* on a non-fermentable carbon source in a defined minimal medium. J Biosci Bioeng 112(1):20–25

Matsuyama A, Arai R, Yashiroda Y, Shirai A, Kamata A, Sekido S, Kobayashi Y, Hashimoto A, Hamamoto M, Hiraoka Y et al (2006) ORFeome cloning and global analysis of protein localization in the fission yeast *Schizosaccharomyces pombe*. Nat Biotechnol 24 (7):841–847

Matsuzawa T, Ohashi T, Hosomi A, Tanaka N, Tohda H, Takegawa K (2010) The gld1+ gene encoding glycerol dehydrogenase is required for glycerol metabolism in *Schizosaccharomyces pombe*. Appl Microbiol Biotechnol 87(2):715–727

Matsuzawa T, Fujita Y, Tohda H, Takegawa K (2012a) Snf1-like protein kinase Ssp2 regulates glucose derepression in *Schizosaccharomyces pombe*. Eukaryot Cell 11(2):159–167

Matsuzawa T, Hara F, Tohda H, Uemura H, Takegawa K (2012b) Promotion of glycerol utilization using ethanol and 1-propanol in *Schizosaccharomyces pombe*. Appl Microbiol Biotechnol 95 (2):441–449

Moreira dos Santos M, Raghevendran V, Kotter P, Olsson L, Nielsen J (2004) Manipulation of malic enzyme in *Saccharomyces cerevisiae* for increasing NADPH production capacity aerobically in different cellular compartments. Metab Eng 6(4):352–363

Mukaiyama H, Tohda H, Takegawa K (2010) Overexpression of protein disulfide isomerases enhances secretion of recombinant human transferrin in *Schizosaccharomyces pombe*. Appl Microbiol Biotechnol 86(4):1135–1143

Neunzig I, Gohring A, Dragan CA, Zapp J, Peters FT, Maurer HH, Bureik M (2012) Production and NMR analysis of the human ibuprofen metabolite 3-hydroxyibuprofen. J Biotechnol 157 (3):417–420

Rhind N, Chen Z, Yassour M, Thompson DA, Haas BJ, Habib N, Wapinski I, Roy S, Lin MF, Heiman DI et al (2011) Comparative functional genomics of the fission yeasts. Science 332 (6032):930–936

Rodriquez-Ruiz J, Belarbi EH, Sanchez JLG, Alsonso DL (1998) Rapid simultaneous lipid extraction and transesterification for fatty acid analyses. Biotechnol Tech 12(9):689–691

Rumbold K, van Buijsen HJ, Gray VM, van Groenestijn JW, Overkamp KM, Slomp RS, van der Werf MJ, Punt PJ (2010) Microbial renewable feedstock utilization: a substrate-oriented approach. Bioeng Bugs 1(5):359–366

Schneider K, Kromer JO, Wittmann C, Alves-Rodrigues I, Meyerhans A, Diez J, Heinzle E (2009) Metabolite profiling studies in *Saccharomyces cerevisiae*: an assisting tool to

prioritize host targets for antiviral drug screening. Microb Cell Fact 8:12

Tarrio N, Becerra M, Cerdan ME, Gonzalez Siso MI (2006) Reoxidation of cytosolic NADPH in *Kluyveromyces lactis*. FEMS Yeast Res 6(3):371–380

Van Urk H, Bruinenberg PM, Veenhuis M, Scheffers WA, Van Dijken JP (1989) Respiratory capacities of mitochondria of *Saccharomyces cerevisiae* CBS 8066 and *Candida utilis* CBS 621 grown under glucose limitation. Antonie Van Leeuwenhoek 56(3):211–220

van Winden WA, Wittmann C, Heinzle E, Heijnen JJ (2002) Correcting mass isotopomer distributions for naturally occurring isotopes. Biotechnol Bioeng 80(4):477–479

Wittmann C, Heinzle E (1999) Mass spectrometry for metabolic flux analysis. Biotechnol Bioeng 62(6):739–750

Yang TH, Frick O, Heinzle E (2008) Hybrid optimization for ^{13}C metabolic flux analysis using systems parametrized by compactification. BMC Syst Biol 2:29

Yang TH, Bolten CJ, Coppi MV, Sun J, Heinzle E (2009) Numerical bias estimation for mass spectrometric mass isotopomer analysis. Anal Biochem 388(2):192–203

Yu KO, Jung J, Kim SW, Park CH, Han SO (2012) Synthesis of FAEEs from glycerol in engineered *Saccharomyces cerevisiae* using endogenously produced ethanol by heterologous expression of an unspecific bacterial acyltransferase. Biotechnol Bioeng 109 (1):110–115